ELSEVIER

NeuroImage

www.elsevier.com/locate/ynimg
NeuroImage 25 (2005) 278–286

Atlas-guided non-uniform attenuation correction in cerebral 3D PET imaging

Marie-Louise Montandon and Habib Zaidi*

Division of Nuclear Medicine, Geneva University Hospital, CH-1211 Geneva 4, Switzerland

Received 27 August 2004; revised 5 November 2004; accepted 15 November 2004
Available online 17 January 2005

Photon attenuation in tissues is the primary physical degrading factor limiting both visual qualitative interpretation and quantitative analysis capabilities of reconstructed Positron Emission Tomography (PET) images. This study investigates the implementation and applicability of transmission atlas-guided attenuation correction in cerebral 3D PET imaging, thus eliminating the need for acquisition of a measured transmission scan. Patient-specific attenuation map is derived by anatomic standardization through nonlinear warping of a stereotactic transmission template obtained by averaging 11 scans of normal subjects. This template is coregistered to a specially designed tracer-specific ^{18}F-[FDG] template constructed by scanning 17 normal subjects in resting condition during tracer uptake in a dark room. This emission template is first coregistered and spatially normalized to preliminary PET images of subjects corrected for scatter and attenuation using an approximate calculated method. The resulting transformation matrices are recorded and re-applied to the transmission template. The derived attenuation map is then forward projected to generate attenuation correction factors to be used for correcting the subjects' PET data. Twelve cerebral clinical studies are used for evaluation of the developed attenuation correction technique as compared to the standard pre-injection measured transmission-based method used in clinical routine. Statistical Parametric Mapping (SPM2) analysis is used to assess significant differences between images obtained using both techniques. The subjective qualitative assessment shows no significant visual differences between atlas-guided and transmission-based attenuation correction methods. However, the quantitative voxel-based analysis comparing atlas-guided to transmission-based attenuation corrections suggest that regional brain metabolic activity increases significantly bilaterally in the superior frontal and precentral gyri, in addition to the left middle temporal gyrus and the left frontal lobe. Conversely, activity decreases in the corpus callosum in the left parasagittal region. A new non-uniform attenuation correction method is thus proposed, which is suitable for both research and clinical routine applications in 3D brain PET imaging on a transmissionless PET scanner or when a patient-specific transmission scan is not available.

Keywords: PET; Attenuation correction; Brain imaging; Statistical parametric mapping

Introduction

Functional brain imaging using single-photon emission computed tomography (SPECT) and positron emission tomography (PET) has steadily gained importance both in clinical setting and research environment over the past few years. Reliable subjective qualitative visual interpretation and accurate objective quantitative analysis of functional brain images rely heavily on the intrinsic performance parameters of the PET scanner and the computational models used to correct the data for physical degrading factors. There is in general a consensus among the nuclear medicine community that photon attenuation is the dominant physical degrading factor besides contribution from scattered photons and other associated errors (Zaidi and Sossi, 2004). The scientific community has witnessed an impressive development of computational models for accurate attenuation correction in PET imaging as an increasing number of clinical indications and research applications are being explored.

The accuracy achieved by the attenuation correction procedure is evidently dependent on the rigour followed to derive the attenuation map. Two broad categories of techniques have emerged: calculated methods, which are based on an assumed anatomical model representing the shape and spatial distribution of attenuation coefficients in the head and measured methods, which in general rely on an additional acquisition of a transmission scan using either positron-emitting (^{68}Ga/^{68}Ge) or single-photon emitting (^{137}Cs) radionuclide sources or an X-ray tube on recently developed dual-modality PET/CT imaging systems (Zaidi and Hasegawa, 2003). It has been shown that motion-induced misalignment between pre-injection transmission and emission scans can result in erroneous estimation of regional

* Corresponding author: Fax: +41 22 372 7169.
E-mail address: habib.zaidi@hcuge.ch (H. Zaidi).
Available online on ScienceDirect (www.sciencedirect.com).

1053-8119/$ - see front matter © 2004 Elsevier Inc. All rights reserved.
doi:10.1016/j.neuroimage.2004.11.021

tissue activity concentrations (van den Heuvel et al., 2003). More recently, a new method based on coregistered segmented magnetic resonance imaging (MRI) was proposed for brain imaging (Zaidi et al., 2003). The main motivation behind the development of this method is to achieve accurate attenuation correction with a transmissionless prototype brain PET tomograph. Removal of the transmission scanning component simplifies greatly the complexity of the tomograph's design and acquisition protocols and contributes significantly to lowering the cost of the prototype and the radiation dose delivered to patients and healthy subjects. In fact, the authors are involved within the Computed Imaging for Medical Applications (CIMA) collaboration in the design of a novel and innovative high-resolution Compton-enhanced 3D brain PET tomograph dedicated to brain research[1] (Braem et al., 2004). This concept leads to an image reconstruction which is free of any parallax error and provides a uniform spatial and energy resolution over the whole sensitive volume. Ideally, it was planned that a 3D brain T1-weighted MRI should be acquired for all subjects participating to research protocols prior to the PET scan. It was realized afterwards that for logistic and practical organizational reasons, the MRI is not always available on the hospital picture archiving and communication system (PACS) and thus another alternative for accurate attenuation correction should be sought.

Historically, empiric calculated methods for deriving the attenuation map in functional brain imaging such as the uniform fit-ellipse method and the automated detection of the head contour followed by assignment of known attenuation coefficients (brain and surrounding skull) were proposed and implemented in software supplied by scanner manufacturers to end-users (Zaidi et al., 2004). Their limitations led to the development of more sophisticated models including the automated method computing a 3-component attenuation map (Weinzapfel and Hutchins, 2001) and the inferring anatomy from a head atlas approach (Stodilka et al., 2000). The former generates an estimated skull image by filtered backprojection of the reciprocal of an emission sinogram whose thickness and radius are estimated from profiles extracted from this image. Whereas the latter derives the attenuation map by registering the brain component of a digital head phantom of a single subject (Zubal et al., 1994) with a source distribution having appropriately scaled specific activities of the gray matter, white matter, and ventricles, to a preliminary PET reconstruction and then applying the resulting spatial transformation to the full head atlas. As reported by many investigators, the major limitation of the Zubal head phantom is that the sinus is larger than usual (Arlig et al., 2000; Stodilka et al., 2000; Zaidi et al., 2004). The method presented in this work further extends this approach and improves its robustness by constructing both transmission and tracer-specific emission atlases based on average patient populations rather than relying on an atlas based on a single subject and a hypothetical tracer distribution. The second improvement is related to application of nonlinear warping for anatomic standardization of stereotactic templates and patient images in contrast to simple global rescaling (7 parameters model) procedures used in the previous studies. In the narrow sense of the word, there is a major conceptual difference between anatomic standardization—also called spatial normalization—and coregistration (Senda, 2000). Basically, coregistration aims to match images of a single subject, usually of a different tracer or modality, through a rigid-body transformation. On the other hand, the purpose of anatomic standardization is to transform brain images of individual subjects into a standard brain. Another important difference is that the true solution exists for registration but not for anatomic standardization (Van Laere and Zaidi, 2005). Standardizing patient brain images should therefore be performed with caution (Senda, 2000). The performance of the proposed attenuation correction algorithm is evaluated using clinical data through comparison to the standard procedure used in clinical routine based on measured pre-injection transmission scanning.

[1] Patent application filed under PCT/EP02/07967, International publication number WO 2004/008177 A1.

Materials and methods

Description of algorithm

The proposed attenuation correction algorithm uses an emission and transmission atlases and preliminary PET reconstructions of the subject's brain images to construct a non-uniform attenuation map adapted to the subject anatomy. The main advantage being that the method does not require additional acquisition of a transmission scan and does not rely on the questionable assumption of perfect coregistration between the transmission and emission scans when using a pre-injection transmission scanning protocol. Fig. 1 shows a flow-chart describing the general principles of the method and main steps required to generate a patient-specific attenuation map. The preliminary 3D PET reconstruction includes model-based scatter correction and calculated attenuation compensation since this has been shown to improve registration accuracy (Stodilka et al., 2000). The basic steps used when applying the method consist of the following:

(1) build ^{18}F-[FDG] PET and transmission stereotactic brain templates from normal databases;
(2) acquire ^{18}F-[FDG] 3D brain PET data for each subject;
(3) preliminary 3D PET reconstruction after scatter and uniform fit-ellipse based calculated attenuation corrections;
(4) anatomic standardization of ^{18}F-[FDG] brain PET template to patient PET images;
(5) record spatial transformation matrix for step (4) above;
(6) apply same spatial transformation to transmission template images;
(7) forward project the obtained attenuation map to generate attenuation correction factors (ACFs) by taking the inverse natural logarithm;
(8) transmission atlas attenuation map-guided scatter correction using the single-scatter simulation (SSS) technique;
(9) non-uniform attenuation correction using the coregistered atlas-guided attenuation map;
(10) 3D brain PET reconstruction using the 3DRP reprojection algorithm.

Obviously, the algorithm performance depends strongly on the anatomic standardization procedure used, which is the crucial step of the proposed approach. Several methods for anatomic standardization of brain images have been developed during the last decade. Automated coregistration approaches generally rely on count difference and mutual information cost schemes. This latter cost function is used in the software package of Statistical

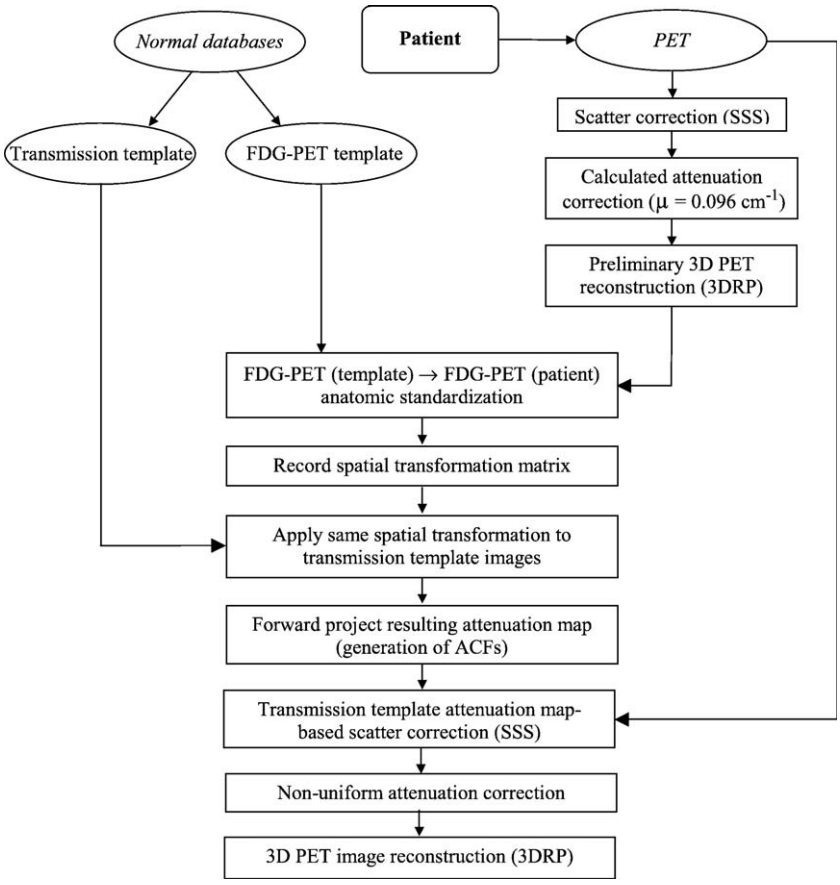

Fig. 1. Flow-chart of the algorithm summarizing the different steps needed to generate an attenuation map from coregistered transmission template images and its use for non-uniform attenuation correction in 3D brain PET imaging. The data are precorrected for scatter using a fast implementation of the single-scatter simulation (SSS) technique followed by attenuation correction and 3D reconstruction using the reprojection (3DRP) analytic algorithm.

Parametric Mapping (SPM) academic freeware (Wellcome Department of Neurology, London, UK) (Friston et al., 2003) and the NEUROSTAT three-dimensional stereotactic surface projection (3D-SSP) method (Department of Internal Medicine, University of Michigan, Ann Arbor, MI, USA) (Minoshima et al., 1994). In this work, anatomic standardization of ^{18}F-[FDG] brain PET stereotactic template to patient PET images was performed using SPM2 software. Anatomic standardization is among the most important pre-processing steps in SPM analysis, which consists in determining the optimum 12-parameter affine transformation followed by nonlinear deformation of brain shape by a linear combination of 3D discrete cosine transform basis functions (Ashburner and Friston, 1999, 2000).

Fig. 2 illustrates the transmission and ^{18}F-[FDG] stereotactic templates used in this study. The tracer-specific ^{18}F-[FDG] PET template was constructed at Gregorio Marañón University Hospital (Madrid, Spain) by scanning 17 normal subjects in resting condition with eyes open during tracer uptake in a dark room (Gispert et al., 2003). This template was built by averaging ^{18}F-[FDG] PET images normalized according to the deformation parameters obtained from MR images. First, PET and MR images are co-registered, and then MR images are normalized to an MRI template. The obtained deformation parameters are finally applied to the subjects' PET images. These normalized images are then averaged and smoothed using 8 mm FWHM Gaussian according to the approach used by Meyer et al. (1999). It is worth emphasizing that the default ^{15}O-[H_2O] template is commonly applied regardless of the specificities of the tracer being used and subjects' conditions (Montandon et al., 2003). The transmission stereotactic template consists of an average image of 11 subjects first registered to the T1-weighted MR images, and spatially transformed using the same transformation similar to the procedure applied for the construction of ^{15}O-[H_2O] PET template supplied with SPM (Friston et al., 2003). Averaged images were smoothed using 8 mm FWHM Gaussian.

PET data acquisition and reconstruction

The study population consisted of 12 women in the early stage of dementia of Alzheimer's type (DAT). Their age ranged from 69 to 81 years (mean ± SD = 75.0 ± 4.71). The 12 subjects were drawn randomly from a large pool of DAT patients participating in a study focusing on the neurofunctional effects of donepezil, a cholinesterase inhibitor, which is a medication used in the treatment of mild to moderate dementia of Alzheimer's patients. This study was approved by the ethical committee of Geneva University Hospital and the Swiss Federal radiation protection authorities. All patients gave their written informed consent for participation in the study protocol.

The method used in clinical routine in our department for attenuation correction is based on the acquisition of an additional pre-injection transmission scan (10 min) using ^{137}Cs single-photon sources. A thermoplastic face mask was used to limit head motion

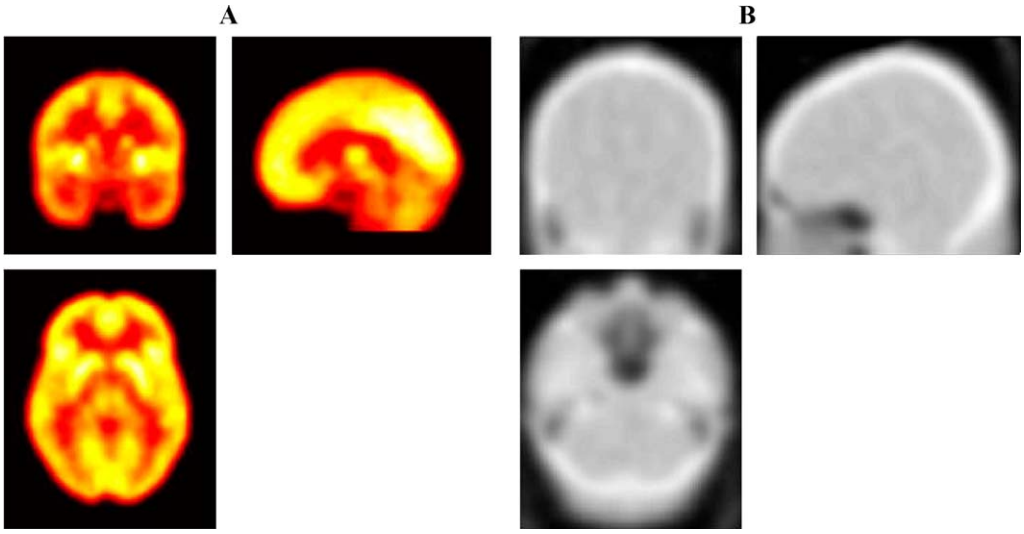

Fig. 2. Illustration of emission and transmission templates used in this study. (A) ^{18}F-[FDG] emission template constructed by averaging ^{18}F-[FDG] PET images of 17 normal subjects normalized according to the deformation parameters obtained from subjects' MR images. (B) Transmission template constructed by averaging 11 normal subjects generated in a similar way to the PET emission template above.

and for accurate repositioning of patients for the emission scan. PET data acquisition (25 min) started 30 min after intravenous injection of approximately 222 MBq of ^{18}F-[FDG] on the ECAT ART continuously rotating partial-ring positron tomograph (CTI/Siemens, Knoxville, TN) operated in fully 3D mode. Images were reconstructed using analytic 3DRP reprojection algorithm (Kinahan and Rogers, 1989) with a maximum acceptance angle corresponding to 17 rings and a span of 7. The default parameters used in clinical routine were applied (Ramp filter, cut-off frequency 0.35 cycles/pixel). The reconstructed images consist of 47 slices with 128×128 resolution and a voxel size set to $1.72 \times 1.72 \times 3.4$ mm^3.

Scatter and attenuation corrections

Scatter correction was performed using a model-based scatter correction algorithm which combines both the emission scan and attenuation map together with the physics of Compton scattering to estimate the scatter distribution (Watson, 2000). The preliminary reconstructions relied on calculated attenuation correction, which was performed by approximating the outline of the head using a slice-dependent ellipse assuming uniform attenuation (μ = 0.096 cm^{-1}) for brain tissues (Zaidi et al., 2004). The atlas-guided attenuation correction matrix is then calculated by forward projection at appropriate angles of the resulting attenuation map. The generated ACFs matrix was then used to correct the emission data. Therefore, the atlas-guided attenuation map served for both scatter and attenuation correction purposes. The measured transmission data are normalized to a slab phantom scan and corrected for scatter and cross-section variation using a log-linear transformation of the attenuation factors (Watson et al., 1997). The images reconstructed with measured attenuation correction served as gold standard for assessment of the newly developed transmission atlas-guided attenuation correction.

Voxelwise statistical image analysis

Voxelwise comparison of PET brain images is a powerful tool compared to manual operator-dependent region of interest (ROI)-based analyses. The different steps involved in the statistical analysis of brain PET images include: coregistration, anatomic standardization, Gaussian smoothing and construction of statistical parametric maps. The images were coregistered and normalized using SPM2 (Friston et al., 2003). A voxelwise paired t test was performed generating a t statistic map with 22 degrees of freedom for the contrast condition effect subsequent to specification of a design matrix. This was then converted to a Z map to assess statistical significance at a P level of 0.05 corrected for multiple comparisons. Changes in regional cerebral glucose metabolism between the images reconstructed using the measured transmission-based and atlas-guided attenuation correction methods were investigated according to the general linear model in each voxel. Proportional scaling was applied by adjusting the mean global activity of each scan to 50 ml/100 ml/min and the threshold of grey matter to 0.80.

Results

A typical plane of a patient brain attenuation map obtained with measured pre-injection transmission and atlas-guided methods are shown in Fig. 3. Horizontal profiles through the sinus cavities and middle of the slice are also shown to demonstrate quantitatively the differences between the different techniques. Note that the typical profile generated by the calculated fit-ellipse method is shown to highlight the limitations of this approach often used in clinical routine in the sense that non-uniformities of the attenuation map are completely ignored. Nevertheless, the sinus cavities on the atlas-guided attenuation map appear slightly larger and the skull base somewhat shifted to the right (at the level of the middle of the slice) compared to the measured transmission method. However, there is good agreement between both methods with respect to estimating skull shape and thickness even if attenuation coefficients are to some extent overestimated on both sides of the sinus for this particular patient. The higher attenuation of the skull and lower attenuation of the nasal sinus are well modeled by the atlas-guided approach.

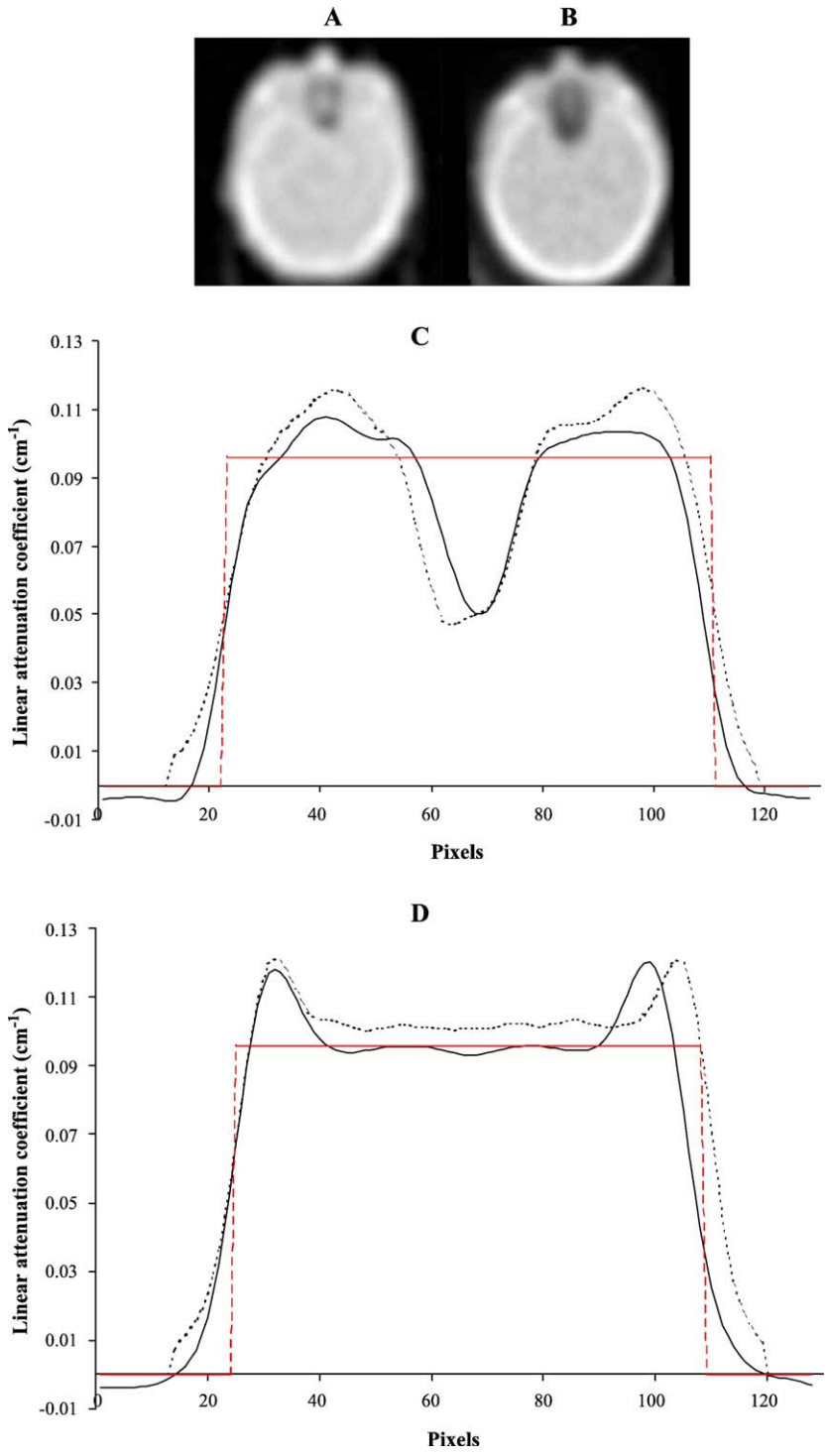

Fig. 3. Illustration of typical plane of patient-specific measured attenuation map using single-photon ^{137}Cs point sources (A), same plane obtained by anatomic standardization through nonlinear warping of Atlas attenuation map (B). The comparison of horizontal profiles between measured (solid line) and transmission template-guided attenuation maps (dotted line) together with the profile obtained using the approximate calculated uniform fit-ellipse-based (dashed line) are also shown at the level of sinus cavities (C) and middle of the slice (D).

Fig. 4 shows brain PET images of a subject as reconstructed using measured transmission-based and atlas-guided attenuation corrections together with horizontal profiles drawn through the thalamus. The qualitative assessment showed no significant visual differences between atlas-guided and transmission-based reconstruction methods. A small but noticeable difference is visible on the horizontal profiles where the transmission atlas-guided approach slightly overestimates the tracer uptake as a result of overestimation of attenuation coefficients (Fig. 3). The transmission map used in this study relied on scans acquired using positron-emitting ^{68}Ga/^{68}Ge rod sources. More appropriate scaling of the transmission template through construction of a template

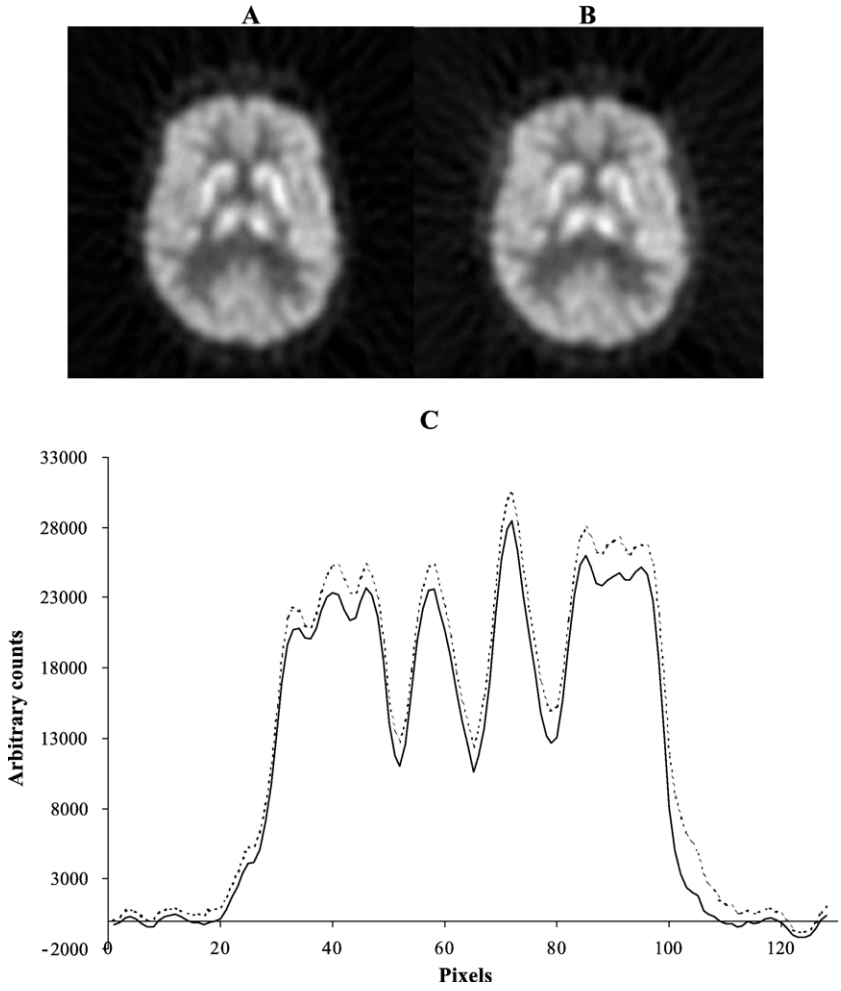

Fig. 4. Comparison of PET image slices of a patient study reconstructed using patient-specific measured transmission-based attenuation correction (A) and transmission template-guided attenuation correction (B). Horizontal profiles comparing the image shown in A (solid line) and B (dotted line) at the level of the thalamus are also shown (C).

based on transmission scans acquired on the same PET scanner used for transmission scanning of the patients equipped with single-photon ^{137}Cs sources should help getting around this problem. As attenuation correction is a multiplicative process, the impact of shifting observed in Fig. 3 is observed on the right side of the profile shown in Fig. 4. Ideally, it would have been desired to acquire several scans per subject to better illustrate the differences between reconstructing the same data with both attenuation correction methods. However, ethical and practical issues make this difficult if not possible to realize in a clinical environment. Care was thus taken to avoid problems of interpreting significance due to an artificially low variance estimate since only one scan per subject were acquired. Fig. 5 shows the mean normalized images reconstructed using atlas-guided and transmission-based attenuation correction algorithms.

Table 1 lists the peaks of the most significant decreases and increases in brain metabolism when images are normalized using the ^{18}F-[FDG] template. The brain structures were determined from the stereotactic coordinates with respect to Talairach and Tournoux atlas (Talairach and Tournoux, 1988). The quantitative statistical voxel-based analysis comparing atlas-guided to transmission-based attenuation corrections suggest that regional brain metabolic activity increases significantly bilaterally in the superior frontal and precentral gyri, in addition to the left middle temporal gyrus and the left frontal lobe. Conversely, activity decreases in the corpus callosum in the left parasagittal region.

Discussion

There are many physiological, biochemical and pharmacological functions of the human brain that can be explored with PET imaging, using for example tracers as ^{18}F-[FDG] to measure the metabolism of glucose, ^{15}O-[H_2O] to assess the rate of blood flow or a large and increasing library of ^{11}C-labeled radioligands to characterize neuroreceptor function. It should be emphasized, however, that many of these applications rely on a solid quantitative foundation, which is highly dependent on the performance characteristics of the PET tomograph and the accuracy of image correction and reconstruction algorithms (Zaidi and Sossi, 2004).

In quantitative functional brain imaging studies, there is always a tension between the desire for more data (MRI, transmission scanning,. . .etc.), which ultimately improves the understanding of the process being studied and the accuracy of the reported results, vs. logistic considerations, including cost, time, PET scanner

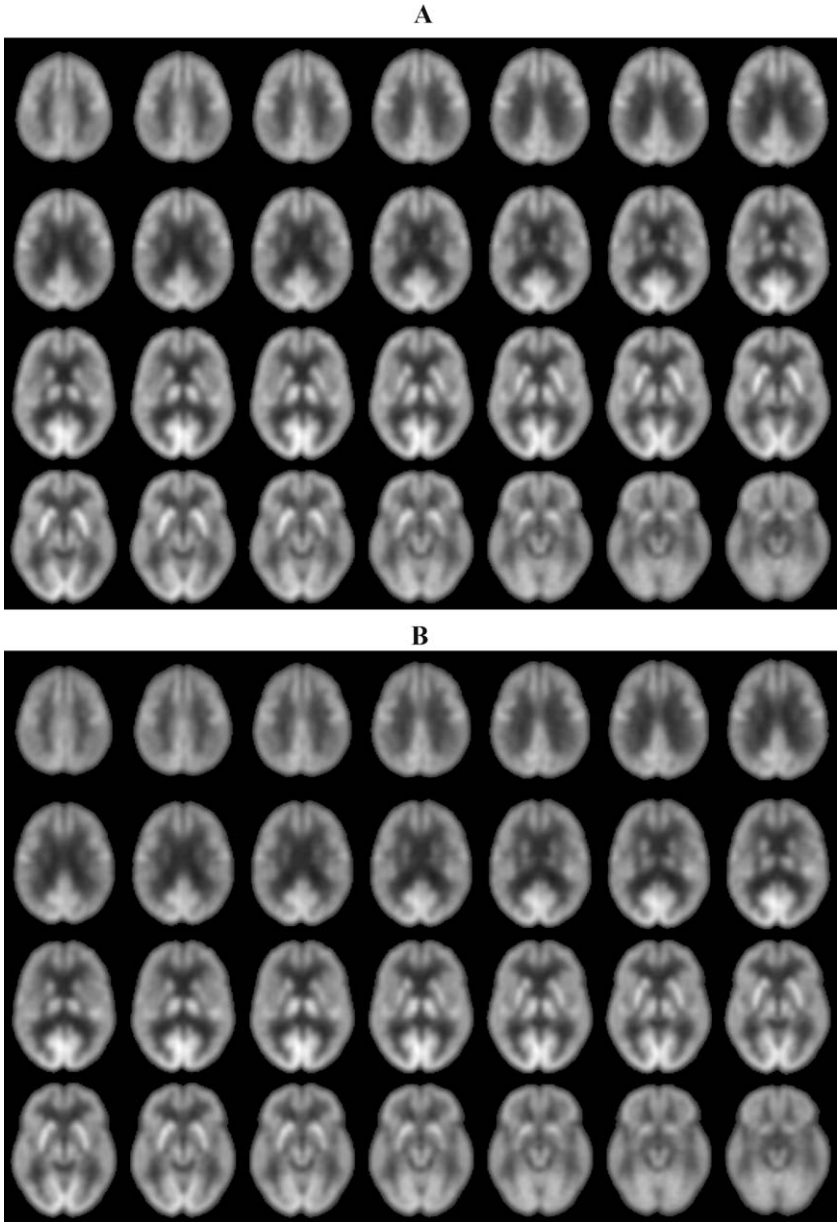

Fig. 5. Mean normalized ^{18}F-[FDG] PET images of the 12 patients used in this study reconstructed using projection data corrected for attenuation using (A) patient-specific measured attenuation map and (B) Atlas-guided derivation of attenuation map.

throughput and patients or healthy volunteers comfort. One must consider what is logistically possible for the staff in a busy clinical PET facility and what is tolerable by the subjects. Head motion and additional time are disadvantageous for transmission-based attenuation correction. However, more widespread applications of PET/CT are addressing these issues effectively. It should be emphasized that in addition to the relatively high cost of these devices, the presence of metallic dental implants can introduce artifacts into brain images, not only when CT is used to determine the attenuation map, but also when a standard positron source is employed for transmission scanning (Goerres et al., 2002). In the clinical setting, it has become standard practice to use simplified imaging protocols compared to the often complex methods developed for research using PET. Much improved high speed, low cost and freely available open source image registration and processing resources are now available and these have made it possible for research groups to design, build and deliver highly sophisticated computational tools for accurate attenuation, and scatter corrections in functional brain imaging (Stodilka et al., 2000; Weinzapfel and Hutchins, 2001; Zaidi et al., 2003).

As mentioned above, our group is part of the CIMA collaboration at CERN, which is actively engaged in the construction of a new high resolution Compton-enhanced PET camera to support ongoing research activities aiming at understanding functionalities of the human brain (Braem et al., 2004). Since it has been decided that this camera will not be equipped with a transmission scanning device to reduce the cost and complexity of the system design, our first attempt to develop a transmissionless attenuation correction method for cerebral 3D PET imaging relied on the use of coregistered T1-weighted MRI of the same subject to derive a

Table 1
Results of statistical parametric mapping analysis comparing PET images reconstructed using patient-specific measured attenuation map and PET images reconstructed using Atlas-guided attenuation map determination

Cerebral structure	Stereotactic coordinates (mm)			Z score
	x	y	z	
Right superior frontal gyrus	8	52	28	+4.74
Left superior frontal gyrus	−16	50	24	+4.09
Left precentral gyrus	−54	−4	36	+3.31
Left middle temporal gyrus	36	6	−38	+2.87
Left frontal lobe	−18	16	−28	+2.26
Right precentral gyrus	56	−4	30	+2.17
Corpus callosum (left parasagittal region)	−2	4	18	−2.10

The stereotactic coordinates corresponding to areas of significant regional increases (+) and decreases (−) in brain metabolism (highest Z score) in a particular cerebral structure with respect to Talairach and Tournoux atlas (Talairach and Tournoux, 1988) are shown.

patient-specific non-uniform attenuation map. We then realized that logistically, MR images are not always readily available online for routine clinical cases and even for research studies.

In this study, we evaluated the feasibility of another transmissionless attenuation correction approach allowing to take into account non-uniformities of the attenuation map through the use of a transmission and tracer-specific emission stereotactic atlases based on average patient populations. This is a major improvement compared to previous studies which relied on an atlas based on a single subject and a hypothetical tracer distribution (Stodilka et al., 2000; Zaidi et al., 2004). It is worth emphasizing that there is a rather important conceptual limitation for this approach, namely the existence of patient-specific anomalies that are evidently not modeled in an atlas obtained from a single or even an average representation of the population. Nevertheless, the method clearly outperforms conventional calculated attenuation correction techniques. Considering the intimate correlation between brain function and morphology, it is very fascinating how accurately normalized brains coincide with each other. The anatomic precision of spatial normalization has been validated with several methods. It has been shown that spatial normalization is most effective when nonlinear transforms are used both for PET perfusion and metabolism and high-resolution anatomical imaging (Sugiura et al., 1999). Van Laere et al. (2001) reported approximately 2-mm template registration accuracy for high-resolution perfusion SPECT or metabolic PET studies. The subjective image quality assessment did not reveal any significant visual differences between the developed method as compared to the measured transmission-based technique considered as the gold standard. The statistical analysis revealed that a small number of cerebral areas show increased or decreased metabolic activity when comparing both attenuation correction methods. The reasons why there are statistically significant differences particularly in these regions are not clear to the authors. It is expected that once these differences are well characterized for healthy and different pathologies of diseased brains, integration of this knowledge by interpreting physicians should allow adequate clinical assessment, interpretation, and quantification of ^{18}F-[FDG] 3D brain PET images.

The fundamental question addressed by this work is: does the global anatomy depicted by normal database really predict individual attenuation map? Anatomic standardization is the most crucial part of the proposed algorithm. Different strategies have been proposed so far with various degrees of success. The development of newer, faster, and more efficient algorithms remains an open research field which requires further research and development efforts. The comparison of SPM and NEUROSTAT anatomic standardization approaches for atrophied brains revealed that both algorithms performed equally well in identifying general patterns of metabolic decrease with DAT patients compared to healthy subjects. However, SPM (SPM99 was used in this study) demonstrated greater inaccuracy and was more sensitive to the presence of atrophy while both methods were prone to artefacts along the ventricular edges (Ishii et al., 2001). A need for further development of both algorithms was indicated.

When imaging patients in a clinical environment, it is worth considering some practical issues with respect to anatomical standardization. In the presence of a focal perfusion or metabolic lesions, automated algorithms attempt to reduce image mismatch between patient image and template at the site of the lesion. This can lead to considerable and inappropriate image distortion, particularly when nonlinear transforms are utilized. A possible solution would be to use cost-function masking, hereby excluding the lesion areas used in the calculation of image difference, so that the lesion does not bias the transformations (Brett et al., 2001). Preliminary investigations using this technique have shown outstanding results when assuming a priori knowledge of the lesion location (Stamatakis et al., 2001). Automated determination of the masked-out regions, when lesion location is not known a priori, remains an open question and needs to be investigated further.

Future work will evaluate the application of other spatial normalization algorithms (e.g., NEUROSTAT) to investigate potential improvements in algorithm performance. The widespread development of age- and gender-specific as well as tracer-specific templates especially for PET radioligands (Van Laere and Zaidi, 2005) such as [^{11}C]-WAY-100635 (serotonin (5HT)-1-A receptors), [^{11}C]-raclopride (striatal dopamine D2 receptors), [^{11}C]-FLB 457 (extrastriatal distribution of D2 receptors), and [^{11}C]-flumazenil (central benzodiazepine receptors) should enable application of the proposed algorithm for children and tracers other than ^{18}F-[FDG].

Conclusion

A new attenuation correction method for 3D brain PET guided by transmission and tracer-specific emission atlases constructed from normal databases representative of average patient populations has been proposed. The method is suitable for either clinical routine and research applications in 3D brain PET imaging on a transmissionless PET scanner or when a transmission scan is not available. Moreover, the removal of the usual pre-injection transmission scan contribute to overall reduction of transmission to emission misregistration errors, radiation absorbed dose and total acquisition time thus increasing patient throughput. Further evaluation of the potential of other anatomic standardization procedures and their applicability to different pathologies of diseased brains remains to be explored.

Acknowledgments

This work was supported by the Swiss National Science Foundation under grant SNSF 3152A0-102143, the National Center of Competence in Research CO-ME and Geneva University Hospital R and D funds under grant PRD-04-1-08. This paper is dedicated to the memory of Prof. F. Terrier (Head of the Department of Radiology, Geneva University Hospital) who sadly passed away this summer.

References

Arlig, A., Gustafsson, A., Jacobsson, L., et al., 2000. Attenuation correction in quantitative SPECT of cerebral blood flow: a Monte Carlo study. Phys. Med. Biol. 45, 3847–3859.

Ashburner, J., Friston, K.J., 1999. Nonlinear spatial normalization using basis functions. Hum. Brain Mapp. 7, 254–266.

Ashburner, J., Friston, K., 2000. Voxel-based morphometry: the methods. NeuroImage 11, 805–821.

Braem, A., Chamizo Llatas, M., Chesi, E., et al., 2004. Feasibility of a novel design of high-resolution parallax-free Compton enhanced PET scanner dedicated to brain research. Phys. Med. Biol. 49, 2547–2562.

Brett, M., Leff, A.P., Rorden, C., Ashburner, J., 2001. Spatial normalization of brain images with focal lesions using cost function masking. NeuroImage 14, 486–500.

Friston, K., Ashburner, J., Heather, J., et al., 2003. Statistical Parametric Mapping (SPM2). Available at www.fil.ion.ucl.ac.uk/spm (The Wellcome Department of Cognitive Neurology, University College London, London).

Gispert, J.D., Pascau, J., Reig, S., et al., 2003. Influence of the normalization template on the outcome of statistical parametric mapping of PET scans. NeuroImage 18, 601–612.

Goerres, G.W., Hany, T.F., Kamel, E., et al., 2002. Head and neck imaging with PET and PET/CT: artefacts from dental metallic implants. Eur. J. Nucl. Med. Mol. Imaging 29, 367–370.

Ishii, K., Willoch, F., Minoshima, S., et al., 2001. Statistical brain mapping of 18F-FDG PET in Alzheimer's disease: validation of anatomic standardization for atrophied brains. J. Nucl. Med. 42, 548–557.

Kinahan, P.E., Rogers, J.G., 1989. Analytic 3D image reconstruction using all detected events. IEEE Trans. Nucl. Sci. 36, 964–968.

Meyer, J.H., Gunn, R.N., Myers, R., Grasby, P.M., 1999. Assessment of spatial normalization of PET ligand images using ligand-specific templates. NeuroImage 9, 545–553.

Minoshima, S., Koeppe, R.A., Frey, K.A., Kuhl, D.E., 1994. Anatomic standardization: linear scaling and nonlinear warping of functional brain images. J. Nucl. Med. 35, 1528–1537.

Montandon, M.-L., Slosman, D.O., Zaidi, H., 2003. Assessment of the impact of model-based scatter correction on 18F-[FDG] 3D brain PET in healthy subjects using statistical parametric mapping. NeuroImage 20, 1848–1856.

Senda, M., 2000. Anatomic standardization, although controversial, finds yet another application. J. Nucl. Med. 41, 1888–1891.

Stamatakis, E.A., Wilson, J.T., Wyper, D.J., 2001. Using lesion masking to facilitate nonlinear alignment of SPECT images. NeuroImage 13, S42.

Stodilka, R.Z., Kemp, B.J., Prato, F.S., et al., 2000. Scatter and attenuation correction for brain SPECT using attenuation distributions inferred from a head atlas. J. Nucl. Med. 41, 1569–1578.

Sugiura, M., Kawashima, R., Sadato, N., et al., 1999. Anatomic validation of spatial normalization methods for PET. J. Nucl. Med. 40, 317–322.

Talairach, J., Tournoux, P., 1988. Co-Planar Atlas of the Human Brain. Thieme Medical Publishers, New York.

van den Heuvel, O.A., Boellaard, R., Veltman, D.J., et al., 2003. Attenuation correction of PET activation studies in the presence of task-related motion. NeuroImage 19, 1501–1509.

Van Laere, K., Zaidi, H., 2005. Quantitative analysis in functional brain imaging. In: Zaidi, H. (Ed.), Quantitative Analysis of Nuclear Medicine Images. Springer, New York. In press.

Van Laere, K., Koole, M., D'Asseler, Y., et al., 2001. Automated stereotactic standardization of brain SPECT receptor data using single-photon transmission images. J. Nucl. Med. 42, 361–375.

Watson, C.C., 2000. New, faster, image-based scatter correction for 3D PET. IEEE Trans. Nucl. Sci. 47, 1587–1594.

Watson, C.C., Jones, W., Brun, T., et al., 1997. Design and performance of a single photon transmission measurement for the ECAT ART. Proc. IEEE Nuclear Science Symposium and Medical Imaging Conference, pp. 1366–1370.

Weinzapfel, B.T., Hutchins, G.D., 2001. Automated PET attenuation correction model for functional brain imaging. J. Nucl. Med. 42, 483–491.

Zaidi, H., Hasegawa, B.H., 2003. Determination of the attenuation map in emission tomography. J. Nucl. Med. 44, 291–315.

Zaidi, H., Sossi, V., 2004. Correction for image degrading factors is essential for accurate quantification of brain function using PET. Med. Phys. 31, 423–426.

Zaidi, H., Montandon, M.-L., Slosman, D.O., 2003. Magnetic resonance imaging-guided attenuation and scatter corrections in three-dimensional brain positron emission tomography. Med. Phys. 30, 937–948.

Zaidi, H., Montandon, M.-L., Slosman, D.O., 2004. Attenuation compensation in cerebral 3D PET: effect of the attenuation map on absolute and relative quantitation. Eur. J. Nucl. Med. Mol. Imaging 31, 52–63.

Zubal, I.G., Harrell, C.R., Smith, E.O., et al., 1994. Computerized 3-dimensional segmented human anatomy. Med. Phys. 21, 299–302.